Coplanar two vortex filaments without change of form

Kazumichi Ohtsuka, Ryuji Takaki, and Shinsuke Watanabe

Citation: Physics of Fluids **16**, 4035 (2004); doi: 10.1063/1.1801371
View online: http://dx.doi.org/10.1063/1.1801371
View Table of Contents: http://scitation.aip.org/content/aip/journal/pof2/16/11?ver=pdfcov
Published by the AIP Publishing

Coplanar two vortex filaments without change of form

Kazumichi Ohtsuka[a)]
Department of Physics, Faculty of Engineering, Yokohama National University, 79-5 Tokiwadai, Hodogaya, Yokohama 240-8501, Japan

Ryuji Takaki[b)]
Faculty of Technology, Tokyo University of Agriculture and Technology, 2-24-16 Nakamachi, Koganei, Tokyo 184-8588, Japan

Shinsuke Watanabe
Department of Physics, Faculty of Engineering, Yokohama National University, 79-5 Tokiwadai, Hodogaya, Yokohama 240-8501, Japan

(Received 29 September 2003; accepted 4 August 2004; published online 5 October 2004)

Shapes of a coplanar vortex pair rotating around a central axis without change of a shape is obtained by solving an equation governing an entanglement motion of a corotating vortex pair. The governing equation, called an entanglement equation, is derived from the Biot-Savart law with an assumption of the local induction. It is shown that the solution exist within a finite range of the radial coordinate perpendicular to the central axis, and that vortex pair takes a shape of horn type or barrel one depending on an intervortex separation at boundary. © *2004 American Institute of Physics*. [DOI: 10.1063/1.1801371]

I. INTRODUCTION

Vortex motions play an important role in high-Reynolds-number flows and in transition processes from laminar flow to turbulent one. Knowledge of fundamental motions of vortices leads to physical understandings of flows and their technological applications such as the aircraft,[1] the semiconductor manufacturing process,[2] the combustion of fuel,[3] and so on. Among various vortex motions, that of vortex filaments constitutes a highly interesting research field, because they show complicated three-dimensional (3D) behavior and still can be studied theoretically. The principle governing their motion is well established, i.e., the Biot-Savart law.[4]

For a single vortex filament in inviscid incompressible fluid with smoothly curved shape, the Biot-Savart law is approximated by the local induction equation.[5] Based on this approximation, some solutions of motions describing a vortex filament without change of form are obtained. The plane sinusoidal filament called Kelvin waves[6] and Euler's Elastica[7] are known as 2D structure of a vortex filament. On the other hand, a helicoidal filament and a vortex soliton[8] are obtained as 3D invariant structures. In addition, Kida[9] gave a solution of a vortex filament which contains all configurations mentioned above and other ones such as closed vortex filament. Fukumoto[10] obtained stationary configurations of a vortex filament in background flows.

Dynamics of a pair of vortex filaments is not investigated enough except for a few cases. The well known cases are motions of parallel and straight vortex pairs with a counterrotating and a corotating filaments. Crow[11] clarified an instability of a counterrotating vortex pair to infinitesimal displacement in a long wave-length region. In addition, Jimenez[12] concluded that a corotating vortex pair is always stable with respect to small perturbations. Dynamics of a curved vortex pair is expected to allow variety of motions, but so far studies of their motions were not systematically carried out, particularly in nonlinear stage. Takaki and Hussain[13] analytically investigated dynamics of a helical pairing on a corotating vortex pair. The present authors showed that a local entanglement on a corotating vortex pair is described by the Korteweg-de Vries (K-dV) equation.[14]

Here arises an interesting problem whether a pair of vortex filament can show a motion with a stationary coplanar structure. This problem may be generalized to include variety of cases with corotating or counterrotating filaments, and with two or more number of filaments. In this paper, we confine ourselves to considering a coplanar structure of a corotating vortex pair with strong deformation. As for the counterrotating case we put a brief comment in the last section.

In Sec. II, we derive an equation governing an entanglement motion of a corotating pair in a cylindrical coordinate system. As a solution of this equation, the helical pairing without a long-wave approximation is given, and is shown to coincide with the long-wave approximation solution obtained by Takaki and Hussain.[13] In Sec. III, two solutions of a coplanar corotating vortex pair are presented by extending the Kida's method.[9] In Sec. IV, discussion is given on 2D configurations of filaments and numerical derivations of vortex shapes. Finally, in Sec. V, conclusions and some remarks are given.

[a)]Present address: Aihara Complexity Modelling Project, ERATO, JST, 45-18 Okayama-cho, Shibuya-ku, Tokyo 151-0065, Japan. Electronic mail: ohtsuka@aihara.jst.go.jp
[b)]Present address: Graduate School, Kobe Design University, 8-1-1 Gakuen-nishimachi, Nishi-ku, Kobe 651-2196, Japan. Telephone: +81-78-794-5263. Electronic mail: takak-ir@kobe-du.ac.jp

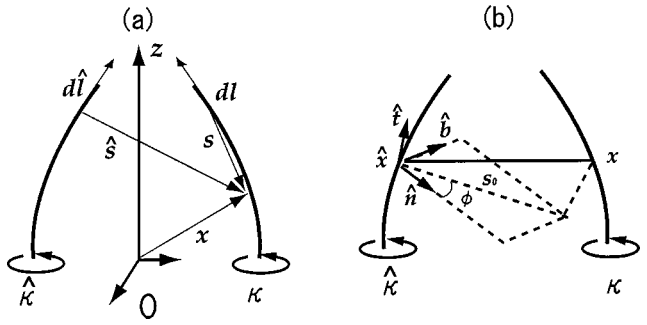

FIG. 1. (a) Definitions of $\mathbf{x}$, $\mathbf{s}$, $\hat{\mathbf{s}}$, $d\mathbf{l}$, and $d\hat{\mathbf{l}}$. (b) Definitions of geometrical parameters s_0 and ϕ.

II. ENTANGLEMENT EQUATION WITH A CYLINDRICAL COORDINATE SYSTEM

A. Entanglement equation

We give a brief introduction of a basic equation governing the motion of a pair of corotating vortex filaments interacting with each other (derivation of this equation is given in Ref. 13). Each vortex filament deforms owing to the effect of the other parts of the same filament and the other filament (the second filament), both of which are described by the Biot-Savart law. The fluid velocity $\mathbf{u}(\mathbf{x})$ at position $\mathbf{x}=(x,y,z)$ on the first filament is expressed by a superposition of these effects as follows:

$$\mathbf{u}(\mathbf{x}) = -\frac{\kappa}{4\pi}\int \frac{\mathbf{s}\times d\mathbf{l}}{s^3} - \frac{\hat{\kappa}}{4\pi}\int \frac{\hat{\mathbf{s}}\times d\hat{\mathbf{l}}}{s^3}, \tag{1}$$

where the first and the second integrals describe the induced velocities from the first and the second filaments, respectively (see Fig. 1). Here κ, $d\mathbf{l}$, and $\mathbf{s}$ represent the circulation, the line segment of the filament, and the vectorial distance from a point on the first filament to the point $\mathbf{x}$. The quantities with hats indicate those concerned to the second filament.

Expression by line integrals in Eq. (1) is valid under the assumptions that the fluid is invisid and unbounded by any solid wall, and that the vortex core size is very small compared to the radius of curvature of the filaments and the mutual distance of them. We further impose here an assumption of symmetry, that is, the two vortex filaments are located at symmetric positions and are deformed symmetrically with respect to the z axis. Then the position $\mathbf{x}$ on the first filament and the corresponding position $\hat{\mathbf{x}}$ on the second filament are related by $\hat{x}=-x$, $\hat{y}=-y$, and $\hat{z}=z$. In order to carry out the integrations in Eq. (1), we introduce two length scales L and L^* which indicate ranges of integrations mainly contributing the first and the second integrations. These scales are assumed to be much larger than the core sizes of filaments and a typical length s_0 between the filaments. Then, the integrations are approximated by those from $-L$ to $-\sigma$ and from σ to L for the first integral of Eq. (1), and from $-L^*$ to L^* for the second one, where σ is a cut-off distance with the same order of magnitude as the core radii. These integrations are made directly, and we have the following local induction approximation (LIA) of Eq. (1):

$$\frac{\partial \mathbf{x}}{\partial t} = \frac{\kappa A}{4\pi\rho}\mathbf{b} + \frac{\hat{\kappa}}{2\pi s_0}(\hat{\mathbf{b}}\cos\phi - \hat{\mathbf{n}}\sin\phi)\left(1+\frac{1}{2}\frac{s_0}{\hat{\rho}}\cos\phi\right), \tag{2}$$

$$A = \ln\frac{Ls_0}{L^*\sigma},$$

where $\mathbf{n}$, $\mathbf{b}$, ρ, and ϕ denote, respectively, the normal vector, the binormal vector, the radius of curvature of the first filaments at the point $\mathbf{x}$, and the angle between a projection of $(\mathbf{x}-\hat{\mathbf{x}})$ to $\hat{\mathbf{n}}\hat{\mathbf{b}}$ plane and $\hat{\mathbf{n}}$ (see Fig. 1). The lengths L and L^* are assumed to have the same order of magnitude as the radii of curvatures of the vortex filaments, so that we regard A as depending on s_0/σ.

So far is an explanation already in Ref. 13, and we proceed further to rewrite Eq. (2) in a cylindrical coordinate system, $\mathbf{x}=(r,\theta,z)$, we have

$$\begin{aligned}\frac{\partial \mathbf{x}}{\partial t} &= A\{(r\theta_s z_{ss} - 2r_s\theta_s z_s - r\theta_{ss}z_s)\mathbf{e}_r + (r_{ss}z_s - r\theta_s^2 z_s \\ &\quad - r_s z_{ss})\mathbf{e}_\theta + (2r_s^2\theta_s + rr_s\theta_{ss} - rr_{ss}\theta_s + r^2\theta_s^3)\mathbf{e}_z\} \\ &\quad - \left\{\frac{1-r(r_{ss}-r\theta_s^2)}{r(1-r_s^2)}\right\}(-r\theta_s\mathbf{e}_z - z_s\mathbf{e}_\theta),\end{aligned} \tag{3}$$

where we have assumed $\kappa=\hat{\kappa}$, $\mathbf{e}_r$, $\mathbf{e}_\theta$, $\mathbf{e}_z$ are unit vectors in the r, θ, and z directions. The subscripts of coordinates (r,θ,z) indicate the partial differentiation with respect to the distance s along the filament. Note that for symmetric configurations of filaments $(\hat{\mathbf{n}},\hat{\mathbf{b}})$ are related to $(\mathbf{n},\mathbf{b})$ and $\hat{\rho}=\rho$. The coordinates s, r, and z have been normalized by the scale R which indicates the distance from the z axis to the vortex filaments and the time t is normalized by the period $4\pi R^2/\kappa$ with which a straight vortex pair makes one rotation around each other.

In deriving Eq. (3), we have used the following expressions of quantities in the cylindrical coordinates:

$$\frac{1}{\rho}\hat{\mathbf{n}} = \hat{\mathbf{x}}_{ss} = [-r_{ss}+r\theta_s^2, -(2r_s\theta_s + r\theta_{ss}), z_{ss}],$$

$$\begin{aligned}\frac{1}{\rho}\hat{\mathbf{b}} = \hat{\mathbf{x}}_s\times\hat{\mathbf{x}}_{ss} &= \{(r\theta_s z_{ss} - 2r_s\theta_s z_s - r\theta_{ss}z_s)\mathbf{e}_r + (r_{ss}z_s \\ &\quad - r\theta_s^2 z_s - r_s z_{ss})\mathbf{e}_\theta + (2r_s^2\theta_s + rr_s\theta_{ss} \\ &\quad - rr_{ss}\theta_s + r^2\theta_s^3)\mathbf{e}_z\},\end{aligned}$$

$$|s_0|^2 = 4r^2(r^2\theta_s^2 + z_s^2) = 4r^2(1-r_s^2),$$

$$|\mathbf{x}_s|^2 = |\mathbf{t}|^2 = r_s^2 + r^2\theta_s^2 + z_s^2 = 1,$$

$$(\mathbf{x}-\hat{\mathbf{x}})\times\hat{\mathbf{t}} = \begin{pmatrix}\mathbf{e}_r & \mathbf{e}_\theta & \mathbf{e}_z \\ 2r & 0 & 0 \\ -r_s & -r\theta_s & z_s\end{pmatrix} = -2rz_s\mathbf{e}_\theta - 2r^2\theta_s\mathbf{e}_z,$$

$$\hat{\mathbf{b}}\cos\phi - \hat{\mathbf{n}}\sin\phi = -\frac{(\mathbf{x}-\hat{\mathbf{x}})\times\hat{\mathbf{t}}}{s_0} = \frac{2rz_s\mathbf{e}_\theta + 2r^2\theta_s\mathbf{e}_z}{s_0},$$

$$\frac{1}{\rho}\cos\phi = (\mathbf{x}-\hat{\mathbf{x}})\left(\frac{1}{\rho}\hat{\mathbf{n}}\right)$$
$$= 2r\mathbf{e}_r\,\hat{\mathbf{x}}_{ss} = 2r(-r_{ss}+r\theta_s^2)$$
$$= -2r(r_{ss}-r\theta_s^2),$$

where **t** expresses a tangent vector on the first filament.

B. Dynamics of helical pairing without a long-wave approximation

In this section, we derive a dispersion relation of helical pairing without a long-wave approximation, and show that this dispersion relation agrees with the relation obtained by Takaki and Hussain[13] in the long-wave limit.

For a periodic helical pairing with a wave number k, we can assume the solution of the following type:

$$\mathbf{x}(s,t) = R_0\{\cos\theta\mathbf{e}_x + \sin\theta\mathbf{e}_y\} + Z\mathbf{e}_z, \tag{4}$$

$$\theta(s,t) = \frac{1}{(R_0^2+b^2)^{1/2}}s + \omega_\theta t, \tag{5}$$

$$Z(s,t) = \frac{b}{(R_0^2+b^2)^{1/2}}s + V_z t, \tag{6}$$

where R_0 is the radius of the helix, $b=1/k$ is the pitch of the helix, ω_θ is the angular frequency of the material motion in the θ direction, and V_z is the material velocity in the z direction. Substituting Eqs. (4)–(6) into Eq. (3), we have

$$R_0\omega_\theta\mathbf{e}_\theta + V_z\mathbf{e}_z = A\left\{-\frac{R_0 b}{(\sqrt{R_0^2+b^2})^3}\mathbf{e}_\theta + \frac{R_0^2}{(\sqrt{R_0^2+b^2})^3}\mathbf{e}_z\right\}$$
$$+\frac{1}{R_0^2}\left(\frac{R_0 b}{\sqrt{R_0^2+b^2}}\mathbf{e}_\theta + \frac{R_0^2}{\sqrt{R_0^2+b^2}}\mathbf{e}_z\right)$$
$$\times\left[1+\frac{R_0^2}{R_0^2+b^2}\right]. \tag{7}$$

Consequently, we obtain

$$\omega_\theta = -\frac{Ab}{(\sqrt{R_0^2+b^2})^3} + \left(\frac{b}{R_0^2\sqrt{R_0^2+b^2}}\right)\left[1+\frac{R_0^2}{R_0^2+b^2}\right],$$

and

$$V_z = \frac{AR_0^2}{(\sqrt{R_0^2+b^2})^3} + \left(\frac{1}{\sqrt{R_0^2+b^2}}\right)\left[1+\frac{R_0^2}{R_0^2+b^2}\right].$$

In order to obtain the dispersion relation, we obtain a phase velocity v_z of the helical vortex in the z direction. Contribution to the phase velocity of the rotation of the helical vortex, say v_{vz}, is given by the product of ω_θ and $-b$ as follows:

$$v_{vz} = \frac{Ab^2}{(\sqrt{R_0^2+b^2})^3} - \frac{1}{R_0^2}\left(\frac{b^2}{\sqrt{R_0^2+b^2}}\right)\left[1+\frac{R_0^2}{R_0^2+b^2}\right]. \tag{8}$$

By adding v_{vz} to the material velocity V_z in Eq. (7), we have the following phase velocity of the filaments in helical pairing and hence angular frequency $\omega=v_z k$ of the helical shape rotation:

$$v_z = \frac{Ak}{\sqrt{1+R_0^2k^2}} + \left(\frac{k}{\sqrt{1+R_0^2k^2}}\right)\left[1-\frac{1}{R_0^2k^2}\right]$$
$$\times\left[1+\frac{R_0^2k^2}{1+R_0^2k^2}\right], \tag{9}$$

$$\omega = \frac{Ak^2}{\sqrt{1+R_0^2k^2}} + \left(\frac{k^2}{\sqrt{1+R_0^2k^2}}\right)\left[1-\frac{1}{R_0^2k^2}\right]$$
$$\times\left[1+\frac{R_0^2k^2}{1+R_0^2k^2}\right]. \tag{10}$$

Note that Eq. (10) is a dispersion relation without a long-wave approximation. The long-wave approximation of Eq. (10), obtained as a limit $R_0^2k^2\to 0$, is

$$\omega = \left(A+\frac{1}{2}\right)k^2 - \frac{1}{R_0^2}. \tag{11}$$

This relation coincides with the dispersion relation obtained by Takaki and Hussain.[13]

C. Kida's method and two vortex filaments

For our purpose to obtain a coplanar shape of a corotating vortex pair, we need to apply the method proposed by Kida.[9] In this section, we extend this method to include the case of corotating vortex filaments. Kida assumed that dynamics of a vortex filament without change of form is reduced to the superposition of the three kinds of motion,

$$\frac{\partial\mathbf{x}}{\partial t} = -C\frac{\partial\mathbf{x}}{\partial\xi} + \Omega\mathbf{e}_z\times\mathbf{x} + V\mathbf{e}_z, \tag{12}$$

$$\xi = s - Ct, \tag{13}$$

where C, Ω, and V represent a speed of the slipping motion along the filament itself, an angular velocity around the z axis, and a speed of the translational motion parallel to the z axis. Note that the induced velocity in the LIA for a single vortex filament is always perpendicular to a vortex filament. Hence, elongation of filament or axial flow does not appear. Equation (12) has a group of solutions expressed as

$$\mathbf{x} = r(\xi)\mathbf{e}_r(\xi,t) + [z(\xi)+Vt]\mathbf{e}_z, \tag{14}$$

where a unit vector in the radial direction $\mathbf{e}_r$ is defined by

$$\mathbf{e}_r = \cos[\theta(\xi)+\Omega t]\mathbf{e}_x + \sin[\theta(\xi)+\Omega t]\mathbf{e}_y. \tag{15}$$

This group includes the solutions of the vortex soliton, the Euler's Elastica, the helicoidal vortex, and so on, which are obtained by substituting Eqs. (12)–(15) into the self-induced equation [for a single vortex filament Eq. (2) without the second term in the right-hand side]. This solution is called here a Kida class.

For the case of a corotating vortex pair with stationary shapes it can express the motion also by the use of Eq. (12). From the dimensionless form of Eqs. (2) and (12), we have

$$-C\frac{\partial \mathbf{x}}{\partial \xi}+\Omega \mathbf{e}_z\times \mathbf{x}+V\mathbf{e}_z=A\left(\frac{\mathbf{b}}{\rho}\right)+\left[\frac{2(\hat{\mathbf{b}}\cos\phi-\hat{\mathbf{n}}\sin\phi)}{s_0}\right]\times\left(1+\frac{1}{2}\frac{s_0}{\hat{\rho}}\cos\phi\right). \tag{16}$$

By rewriting this equation in a cylindrical coordinates, and taking vector product with $\partial \mathbf{x}/\partial\xi$, we have

$$(\Omega r z_\xi - V r\theta_\xi)\mathbf{e}_r + V r_\xi \mathbf{e}_\theta - \Omega r r_\xi \mathbf{e}_z = A\left(\frac{\mathbf{n}}{\rho}\right)-\left[\frac{1-r(r_{\xi\xi}-r\theta_\xi^2)}{r(1-r_\xi^2)}\right][(-z_\xi^2+r^2\theta_\xi^2)\mathbf{e}_r + (-rr_\xi\theta_\xi)\mathbf{e}_\theta + r_\xi z_\xi \mathbf{e}_z]. \tag{17}$$

Since $\partial/\partial s=\partial/\partial\xi$ [see Eq. (13)], the right-hand side of Eq. (3) does not change its form through the variable transformation from s to ξ. In deriving Eq. (17), we have used the relations,

$$\mathbf{e}_z\times\mathbf{x}=\begin{pmatrix}\mathbf{e}_r & \mathbf{e}_\theta & \mathbf{e}_z\\ 0 & 0 & 1\\ r & 0 & z+Vt\end{pmatrix}=r\mathbf{e}_\theta,$$

$$(\mathbf{e}_z\times\mathbf{x})\times\mathbf{x}_s=\begin{pmatrix}\mathbf{e}_r & \mathbf{e}_\theta & \mathbf{e}_z\\ 0 & r & 0\\ r_\xi & r\theta_\xi & z_\xi\end{pmatrix}=rz_\xi\mathbf{e}_r-rr_\xi\mathbf{e}_z,$$

$$\mathbf{e}_z\times\mathbf{x}_s=\begin{pmatrix}\mathbf{e}_r & \mathbf{e}_\theta & \mathbf{e}_z\\ 0 & 0 & 1\\ r_\xi & r\theta_\xi & z_\xi\end{pmatrix}=-r\theta_\xi\mathbf{e}_r+r_\xi\mathbf{e}_\theta,$$

$$(\mathbf{e}_r\times\hat{\mathbf{x}}_s)=\begin{pmatrix}\mathbf{e}_r & \mathbf{e}_\theta & \mathbf{e}_z\\ 1 & 0 & 0\\ -r_\xi & -r\theta_\xi & z_\xi\end{pmatrix}=-z_\xi\mathbf{e}_\theta-r\theta_\xi\mathbf{e}_z,$$

$$(\mathbf{e}_r\times\hat{\mathbf{x}}_s)\times\mathbf{x}_s=\begin{pmatrix}\mathbf{e}_r & \boldsymbol{\theta} & \mathbf{e}_z\\ 0 & -z_\xi & -r\theta_\xi\\ r_\xi & r\theta_\xi & z_\xi\end{pmatrix}=(r^2\theta_\xi^2-z_\xi^2)\mathbf{e}_r-rr_\xi\theta_\xi\mathbf{e}_\theta+r_\xi z_\xi\mathbf{e}_z.$$

Comparison of each component of Eq. (17) leads to the following three equations:

$$\mathbf{e}_r:(\Omega r z_\xi - V r\theta_\xi)=A(r_{\xi\xi}-r_\xi\theta_\xi^2)-\left[\frac{1-r(r_{\xi\xi}-r\theta_\xi^2)}{r(1-r_\xi^2)}\right]\times(-z_\xi^2+r^2\theta_\xi^2), \tag{18}$$

$$\mathbf{e}_\theta:Vr_\xi=A(2r_\xi\theta_\xi+r\theta_{\xi\xi})-\left[\frac{1-r(r_{\xi\xi}-r\theta_\xi^2)}{r(1-r_\xi^2)}\right](-rr_\xi\theta_\xi), \tag{19}$$

$$\mathbf{e}_z:-\Omega r r_\xi=Az_{\xi\xi}-\left[\frac{1-r(r_{\xi\xi}-r\theta_\xi^2)}{r(1-r_\xi^2)}\right]r_\xi z_\xi. \tag{20}$$

Equations (18)–(20) and a constraint

$$|\mathbf{x}_s|^2=|\mathbf{t}|^2=r_\xi^2+r^2\theta_\xi^2+z_\xi^2=1, \tag{21}$$

constitute the basic equations for a corotating vortex pair. Here we mention that Eqs. (18)–(20) coincide with the basic equations proposed by Kida, if we neglect the induced velocity from the second filament [neglecting the second terms in the right-hand sides in Eqs. (18)–(20) and replacing the parameter $A\to A'=\ln(L/\sigma)$].

III. COPLANAR SOLUTIONS OF TWO VORTEX FILAMENTS

A. Governing equation and a solution in a long wave limit

For a coplanar configuration of a corotating vortex pair at an instant when they lie on the plane with $\theta_\xi=0$, we obtain the following equations from Eqs. (18)–(20):

$$\mathbf{e}_r:\Omega r z_\xi=Ar_{\xi\xi}-\left[\frac{1-rr_{\xi\xi}}{r(1-r_\xi^2)}\right](-z_\xi^2),$$

$$\mathbf{e}_\theta:Vr_\xi=0, \tag{22}$$

$$\mathbf{e}_z:-\Omega r r_\xi=Az_{\xi\xi}-\left[\frac{1-r(r_{\xi\xi})}{r(1-r_\xi^2)}\right]r_\xi z_\xi. \tag{23}$$

These equations can be simplified by the use of relations obtained from Eq. (21) for $\theta_\xi=0$, i.e.,

$$z_\xi=\sqrt{1-r_\xi^2}, \tag{24}$$

$$z_\xi z_{\xi\xi}=-r_\xi r_{\xi\xi}. \tag{25}$$

Substituting Eqs. (24) and (25) into Eq. (23), we have

$$\Omega r^2\sqrt{1-r_\xi^2}=1+(A-1)rr_{\xi\xi}. \tag{26}$$

If r is a constant through the all range of ξ, Eq. (26) reduces to

$$\Omega=\frac{1}{r^2}. \tag{27}$$

This dimensionless angular velocity coincides with that of a rectilinear corotating vortex pair.

Here we assume that the filaments are nearly parallel to the z axis, so that the derivatives with respect to ξ are small quantities denoted by $O(\epsilon)$ (a long-wave approximation). Expanding the root in the left-hand side of Eq. (26) with respect to r_ξ^2 and estimating up to the order $O(\epsilon^2)$, we have

$$\Omega r^2-\frac{\Omega r^2 r_\xi^2}{2}=1+(A-1)rr_{\xi\xi}. \tag{28}$$

This equation can be solved by an exchange of argument and function, i.e., from $r(\xi)$ to $\xi(r)$. By the use of the following relations:

$$r_\xi = \frac{1}{\left(\frac{d\xi}{dr}\right)}, \tag{29}$$

$$r_{\xi\xi} = \frac{d}{d\xi}\left(\frac{1}{\left(\frac{d\xi}{dr}\right)}\right) = \frac{dr}{d\xi}\frac{d}{dr}\left(\frac{1}{\left(\frac{d\xi}{dr}\right)}\right) = \left(\frac{-1}{\left(\frac{d\xi}{dr}\right)^3}\right)\frac{d^2\xi}{dr^2}, \tag{30}$$

Eq. (28) is transformed to

$$\frac{dp}{dr} - \alpha r p = -\beta\left(\Omega r - \frac{1}{r}\right)p^3, \tag{31}$$

where $p = d\xi/dr$ and

$$\alpha = \frac{\Omega}{2(A-1)}, \quad \beta = \frac{1}{(A-1)}.$$

This is the Bernoulli's differential equation, and its solution is obtained in the following way. Assuming $q = p^{-2}$ and substituting this relation into Eq. (31), we have

$$q = \left(\frac{dr}{d\xi}\right)^2 = e^{-\alpha r^2}\left[2\beta\int\left(\Omega r - \frac{1}{r}\right)e^{\alpha r^2}dr\right]$$
$$= [2 - \beta \mathrm{Ei}[\alpha r^2]e^{-\alpha r^2}] \tag{32}$$

where Ei is the exponential integral function defined by

$$\int \frac{1}{r}e^{\alpha r^2}dr = \frac{1}{2}\mathrm{Ei}[\alpha r^2]. \tag{33}$$

From Eq. (32), we have

$$\frac{dr}{d\xi} = \pm\sqrt{2 - \beta \mathrm{Ei}[\alpha r^2]e^{-\alpha r^2}}. \tag{34}$$

The case with minus sign in this equation corresponds to a vortex shape which is an inversion of another case (plus sign) in the z direction. Hence, we can confine ourselves to the case with sign without loss of generality. From Eq. (34)

$$\int \frac{1}{\sqrt{2 - \beta \mathrm{Ei}[\alpha r^2]e^{-\alpha r^2}}}dr = \xi. \tag{35}$$

From Eqs. (24) and (34), we have

$$\frac{dz}{d\xi} = \sqrt{[\beta \mathrm{Ei}[\alpha r^2]e^{-\alpha r^2} - 1]}. \tag{36}$$

On the other hand, since

$$\frac{dz}{d\xi} = \frac{dz}{dr}\frac{dr}{d\xi} = \sqrt{2 - \beta \mathrm{Ei}[\alpha r^2]e^{-\alpha r^2}}\frac{dz}{dr}, \tag{37}$$

Eq. (36) is reduced to a differential equation for $z(r)$:

$$\frac{dz}{dr} = \sqrt{\frac{\beta \mathrm{Ei}[\alpha r^2]e^{-\alpha r^2} - 1}{2 - \beta \mathrm{Ei}[\alpha r^2]e^{-\alpha r^2}}}. \tag{38}$$

The quantity in the root of Eq. (38), containing $\mathrm{Ei}[\alpha r'^2]e^{-\alpha r'^2}$ at the both denominator and numerator, takes positive and negative values depending on r and A. In order that the root remains real, r must be confined in a range with a maximum $r_{\max}$ and a minimum $r_{\min}$. Hence, a coplanar vortex pair described by Eq. (39) has edges at these positions. This equation gives the solution of a coplanar corotating vortex filaments after integration with respect to r,

$$z = \int_{r_{\min}}^{r} \sqrt{\frac{\beta \mathrm{Ei}[\alpha r'^2]e^{-\alpha r'^2} - 1}{2 - \beta \mathrm{Ei}[\alpha r'^2]e^{-\alpha r'^2}}}dr', \tag{39}$$

where we have chosen the origin of z at $r = r_{\min}$. Note again that this solution is valid for a symmetric coplanar vortex pair with the same strength in long-wave deformation. It is worth noting also on a character of the vortex shape. Since the integrand in Eq. (39) is a positive quantity, z is an increasing function of r. Therefore, $dr/d\xi$ and $dz/d\xi$ are always positive, since ξ is the length measured along the vortex filament. The value of dz/dr ranges from zero to infinity, while $dr/d\xi$ and $dz/d\xi$ vary from zero to unity [see Table I and Eq. (21)].

TABLE I. Values of $r_{\min}$, $r_{\max}$, $(dz/dr)_{\max}$, $(dr/d\xi)_{\max}$, $r|_{(dr/d\xi)_{\max}}$, and $r|_{(dz/dr)_{\max}}$ for given values of A based on the long-wave approximation.

A	$r_{\min}$	$r_{\max}$	$(dz/dr)_{\max}$	$(dr/d\xi)_{\max}$	$r\|_{(dr/d\xi)_{\max}}$	$r\|_{(dz/dr)_{\max}}$
1.2	0.43	0.48	∞	1	0.43	0.48
1.3	0.55	0.69	∞	1	0.55	0.69
1.37	0.645	0.965	∞	1	0.645	0.965
1.4	0.683	1.71	0.9	1	0.683	1
1.5	0.819	1.72	0.68	1	0.819	1.06
1.6	0.975	1.69	0.49	1	0.975	1.27
1.7	1.19	1.59	0.25	1	1.19	1.38
1.74	1.4	1.4	0	1	1.4	1.74

On the other hand, we need a precise discussion on the value of $r_{\min}$ as given in the following section.

B. Approximate solution for $A \simeq 1$

We give another approximate solution of coplanar vortex pairs, which is valid for $A \simeq 1$. As mentioned in Sec. II A, $A = \ln(Ls_0/L^*\sigma)$ depends mainly on the ratio of the mutual distance s_0 to the radius σ, since L and L^* are assumed to have the same order. Then, the assumption $A = 1$ ($\simeq \ln e$) indicates that $s_0 : \sigma \simeq 2.718 : 1$. This ratio does not contradict with the initial implicit assumption that the two filaments are separated. However, it seems to violate the condition that their distance is much larger than the core size. However, since the value 2.718 is not very bad, we try to make this assumption and to discuss later the result.

When A is close to unity, Eq. (26) is reduced to

$$\left(\frac{dr}{d\xi}\right)^2 = \left(\frac{dr}{ds}\right)^2 = 1 - \left(\frac{1}{\Omega^2}\right)\frac{1}{r^4}. \tag{40}$$

From Eqs. (24) and (40), we have

$$\left(\frac{dz}{d\xi}\right)^2 = \left(\frac{dz}{ds}\right)^2 = \frac{1}{\Omega^2 r^4}. \tag{41}$$

By the use of Eqs. (40) and (41), we have

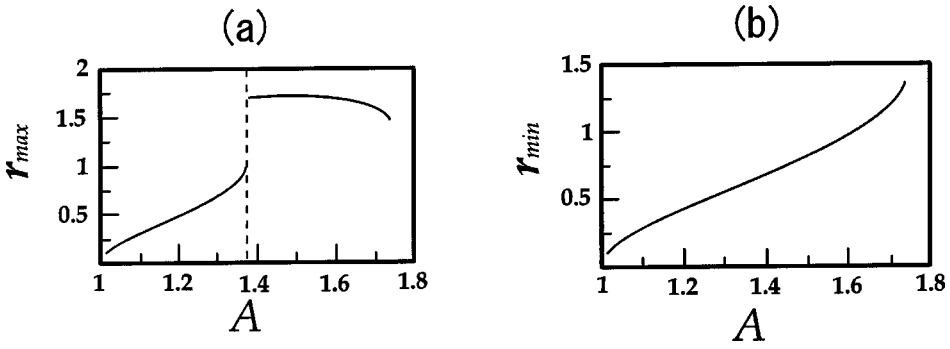

FIG. 2. Dependences of (a) $r_{\max}$ and (b) $r_{\min}$ on the parameter A for $\Omega=1$.

$$dz = \pm \frac{1}{\Omega\sqrt{r^4 - \frac{1}{\Omega^2}}} dr. \tag{42}$$

Introducing a new variable

$$f = \sqrt{r^4 - \frac{1}{\Omega^2}}, \tag{43}$$

Eq. (42) is transformed to

$$dz = \pm \frac{1}{2\Omega\left(f^2 + \frac{1}{\Omega^2}\right)^{3/4}} df. \tag{44}$$

Integrating Eq. (44), we obtain

$$z = \pm \frac{\sqrt{\Omega\left(r^4 - \frac{1}{\Omega^2}\right)}}{2} \left\{ {}_2F_1\left[\frac{1}{2}, \frac{3}{4}, \frac{3}{2}, -\Omega^2\left(r^4 - \frac{1}{\Omega^2}\right)\right]\right\}, \tag{45}$$

where ${}_2F_1$ is a hypergeometric function.

IV. DISCUSSION

A. Configuration of a plane vortex pair in a long-wave approximation

Since we cannot make the integration in Eq. (39) analytically, we try to make it numerically. Let us choose $\Omega=1$ for simplicity. Table I shows the values of $r_{\max}$ and $r_{\min}$ for some values of A. In Fig. 2, $r_{\min}$ and $r_{\max}$ are plotted against A. Some properties of the shapes of a coplanar vortex pair can be derived from Table I, Fig. 2, and numerical results. They are summarized as follows.

(1) The values of $r_{\max}$ (the position of the upper end of the vortex), and $(dz/dr)_{\max}$ vary discontinuously at $A=A_c=1.371$. The quantity $r_{\max}$ takes a maximum value 1.722 at $A=1.505$, while $r_{\min}$ (the position of the lower edge) increases monotonically with A.

(2) When $A \geqslant 1.74$ the integrand in Eq. (39) takes only complex values, and solution of the long-wave approximation cannot exist. Note that Table I shows $r_{\max}-r_{\min}=0$ at $A=1.74$.

(3) The value of $dr/d\xi$ has a maximum value, unity, at $r=r_{\min}$, i.e., filaments are horizontal at the lower end. Behavior of $dz/d\xi=0$ is also seen from Eq. (24).

(4) Vortex filaments show different shapes between cases $A>1.371$ and $A<1.371$.

Shapes of vortex pair are plotted in Fig. 3 for $A=1.371$, 1.4, and 1.5. When $A>1.371$, the vortex pair takes horn-like curves with an inflection point. If $A_c=1.371$, dz/dr becomes infinity at $r=r_{\max}$, and the vortex pair approaches asymptotically to rectilinear filaments parallel to the z axis. On the other hand, if $A \leqslant A_c$, the vortex pair has end points at a finite value of z. However, from the local induction mechanism, the vortex pair can be connected to another pair with inverted shape with respect to z direction [corresponding to the minus sign in Eq. (34)]. This situation is discussed once

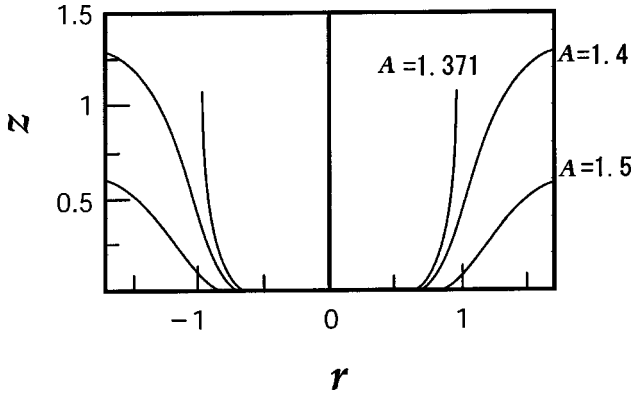

FIG. 3. Theoretical shapes of coplanar vortex pair based on the long-wave approximation for $\Omega=1$, $A=1.371$, 1.4, and 1.5.

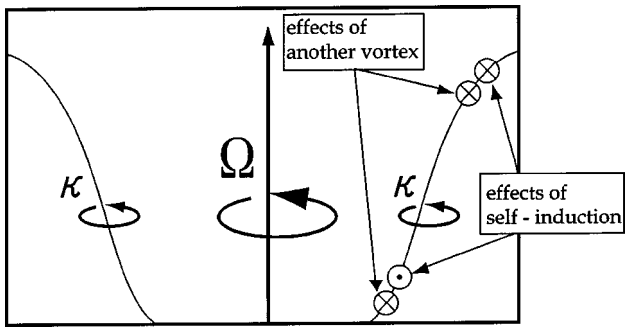

FIG. 4. Rough sketch of the effects of self-induction and another vortex. Circles with dot indicate the induced velocities directed out of the paper (towards readers), while circles with cross indicate the induced velocities directed into the paper (from readers).

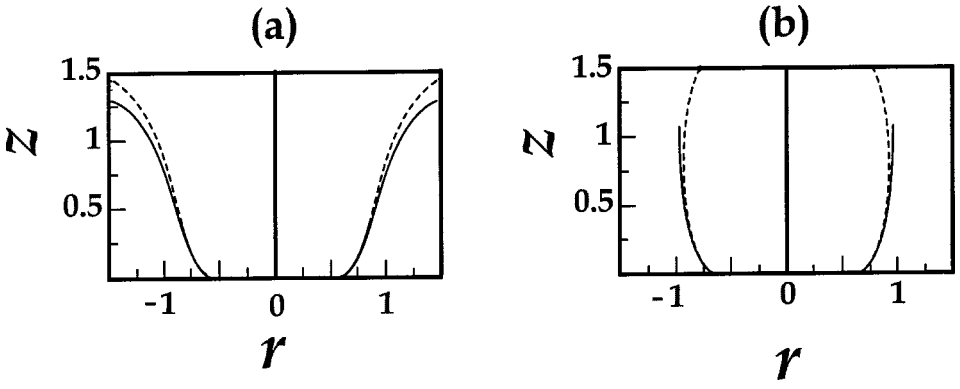

FIG. 5. Comparison of vortex shapes obtained by solving Eq. (26) numerically (broken lines) and by numerical integration of Eq. (39) (solid curves) for $\Omega=1$, (a) $A=1.4$ and (b) $A=1.37$.

more below. However Eq. (39) does not allow the solution to extend above the point with $dz/dr=\infty$ [see Fig. 5(b)].

Here, it is worth noting on how the vortices can be rotated around z axis with uniform angular velocity, for a particular value of $A=1.4$. As shown in Fig. 4, the rotating velocity is a superposition of the effect of self-induction and that of another vortex, and they cancel in lower part while they sum up in upper part. Therefore, if the vortex has an appropriate shape, each part of the vortex has a velocity proportional to r, hence the angular velocity of rotation Ω remains uniform although the vortex separation, $2r$, is not uniform.

Plane configurations obtained from Eq. (39) satisfy the boundary condition, $dr/d\xi=1$ and $dz/d\xi=0$ at $r=r_{\min}$, contradicting with a long-wave approximation $dr/d\xi=O(\epsilon)$. Therefore, we must examine our analysis by returning to Eq. (26) and solving it numerically. This equation was solved by Runge-Kutta method. Note that Eq. (26) contains second-order derivative, and we need to give both values of r and r_ξ at $z=0$. These values are fixed at the same values as those of analytical solutions. The numerical results (broken lines) agree well with the analytical solutions of Eq. (39) (solid lines) for $A=1.4$ [Fig. 5(a)] and $A=1.37$ [Fig. 5(b)]. The barrel-like curve shown in Fig. 5(b) corresponds to the shape connected the solid curve of Fig. 5(b) with inversion of this curve in z direction.

B. Configuration of a plane vortex pair for $A\simeq 1$

We compare shapes of a coplanar vortex pair described by Eq. (45) with numerical result and examine the validity of the assumption $A\simeq 1$ in Sec. III B. Figure 6(a) shows the theoretical shape of the coplanar filaments for $A\simeq 1$ with $\Omega=1$. We solved Eq. (26) numerically for $A=1.01$, 1.1, and 1.4 under the boundary condition, $dr/d\xi=0$ and $dz/d\xi=1$, $r_{\rm ini}$ (a value of r at $z=0$) $=1.01$ at $z=0$. Note that $r_{\rm ini}>1$ from Eq. (40). Results of numerical calculation are shown in Fig. 6(b). This figure indicates that the analytical solution Eq. (45) agrees reasonably well with the numerical result for $A=1.01$. Figure 6(b) shows that straight part of filaments becomes longer as A increases. We can connect these solutions with inverted ones at $z=0$ where filaments are parallel to z axis. Hence, a coplanar filaments with the x-like curve is valid as the curve without change of form.

C. Intervortex separation at boundary

Our analyses mentioned above have revealed various shapes of vortex pair. Parameters that decide the shapes are the value of A, Ω, and the boundary conditions at $z=0$. In this section, we examine how vortex configurations depend on boundary conditions for r and r_ξ at $z=0$ based on numerical solutions of Eq. (26). We assume $\Omega=1$, and treat the same cases as shown in Figs. 5 and 6.

In the case $(r_\xi, z_\xi)=(1,0)$ at $z=0$ (corresponding to Fig. 5), the critical value of r at $z=0$ at which coplaner filaments change their form from barrel-type to horn one denoted by $r_{\rm ini}=r_{C\,\min}$ is shown in Fig. 7. We compare the theoretical shape of Eq. (39) having a lower edge at $(r,z)=(r_{\min},0)$ with a numerical solution of Eq. (26) having initial values of this differential equation, $(r,z)=(r_{\rm ini},0)$. To calculate the second

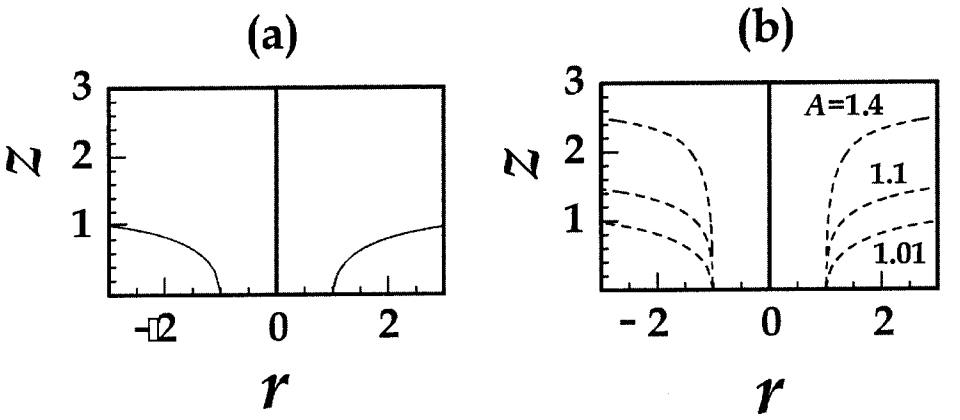

FIG. 6. Comparison of vortex shapes for $A\simeq 1$ and $\Omega=1$. (a) Theoretical shape of coplanar vortex filaments for $A\simeq 1$ described by Eq. (45). (b) Numerical solutions of Eq. (26) for $A=1.01$, 1.1, and 1.4 with $r_{\rm ini}=1.01$. The numerical curve with $A=1.01$ almost coincide with the theoretical curve [Fig. 6(a)].

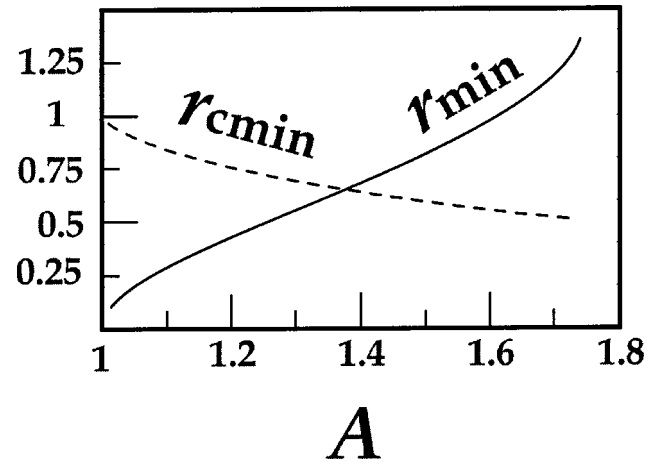

FIG. 7. Dependences of $r_{\min}$ and $r_{C\,\min}$ on the parameter A. The solid curve indicates the values of $r_{\min}$ for A. The broken one indicates $r_{C\,\min}$.

differential equation (26) numerically, we must give an additional condition $(r_\xi, z_\xi)=(1,0)$ at $z=0$ (vortex filaments having the edge parallel to the r axis). Numerical results shows that coplanar filaments change their forms from barrel to horn, when $r_{\rm ini}=r_{C\,\min}$. In Fig. 7, values of $r_{\min}$ and $r_{C\,\min}$ for A are compared. Results of numerical calculations of Eq. (26) indicate that a vortex shape always takes barrel-like curves for all A when $r_{\rm ini}<r_{C\,\min}$. On the other hand, when $r_{C\,\min}\leqslant r_{\rm ini}$, shapes of filaments become horn-like curves. Our analysis in the above section seizes a part of characteristics of plane filaments with initial conditions $r_{\min}<r_{C\,\min}$ when $A\leqslant A_c$ and with $r_{C\,\min}\leqslant r_{\min}$ when $A_c<A$. Then we confirm that these values coincide each other at $A=1.374$, which almost agrees with our former result $A_c=1.371$.

On the other hand, in the case with $(r_\xi, z_\xi)=(0,1)$ at $z=0$ (corresponding to Fig. 6), vortex filaments change its shape depending on whether $r_{\rm ini}>1$ or $r_{\rm ini}<1$. Figure 8 shows numerical solutions of vortex filaments for $r_{\rm ini}=0.999$ and $r_{\rm ini}=1.01$. From Eq. (27), we see that $r_{C\,\min}=1/\sqrt{\Omega}=1$ is the initial intervortex separation which makes rectilinear corotating filaments. This figure indicates that intervortex separation increases (or decreases) with z if $r_{\rm ini}>1$ (or $r_{\rm ini}<1$). This fact corresponds to a transition of vortex shape from a barrel curve to a horn one as shown in Fig. 5. This transition of shapes seems to be analogous to the beginning of a global entanglement of corotating vortex filaments when the intervortex separation deviates from an equilibrium state shown in Sec. V of our previous study.[14]

V. CONCLUSION

In this study, we have derived Eq. (3) as an equation governing an entanglement on a vortex pair in the polar coordinate system, and Eq. (26) as one governing a particular motion of coplanar vortex pair rotating around a central axis without shape change. We have solved the latter equation analytically under the long-wave approximation, and also numerically without this approximation. They are shown to agree well each other. We have shown that coplanar vortex shape varies from a barrel type to a horn one according to the boundary condition at $z=0$. For rectilinear filaments, $r_{C\,\min}$ corresponds to the equilibrium intervortex separation which classifies two kinds of a coplanar shape. Present work can be looked upon as an extension of the past work by Takaki and Hussain[13] in a sense that it has generalized the past work to cover a case without long-wave approximation. It is also an extension of Kida's work,[9] since an effect of another vortex is considered in addition to the self-induction.

Finally, a comment is given on a possibility to observe real coplanar vortex pair as shown in Figs. 3, 5, 6, or 8. These filaments have end points within the fluid at $r=r_{\min}$, which does not occur in real filaments. Note that end points where the vortices are parallel to the z axis are not a problem, because we can connect inverted vortices there. One possibility might be a case where the filaments are attached to a solid wall with an ideal shape so that it does not disturb the flow. A vortex pair with the shape as shown in Fig. 8, for example, may be realized. In fact, Watanabe[15] observed a single stationary 2D vortex filament, with a shape of Euler's Elastica, which was attached to the inside wall of a hemisphere cap. Therefore, Fig. 8(b) could be observed in an ideal container with suitable upper and lower walls. In addition, the boundary conditions for the filaments shown in Fig. 8(a) may be satisfied in a situation where the upper ends of filaments are attached to the outside wall of a hemisphere. However, it is also difficult to construct a container which does not disturb the flow field produced by the filaments. A better interpretation would be to assume that both ends of the filaments are touching the ends of thin rods which are set in fluid rotating around the z axis with the same angular velocity as the filament.

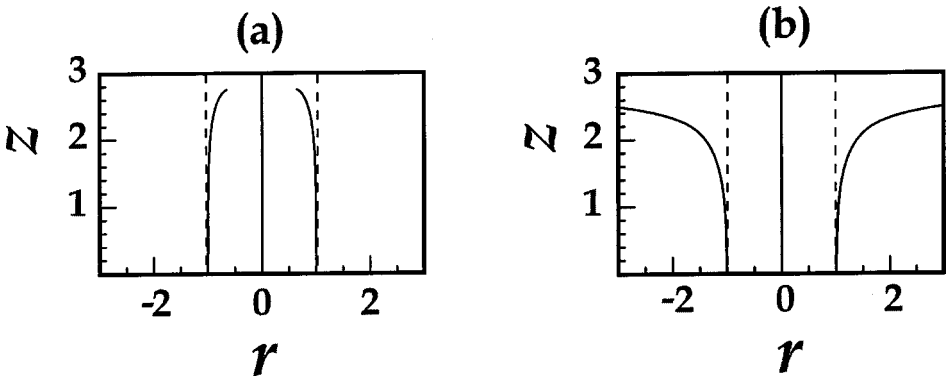

FIG. 8. Dependence of vortex shape on initial value of r for the case $dz/d\xi=0$ at $z=0$ and $A=1.4$. 2D configurations of a vortex pair plotted for the conditions (a) $r_{\rm ini}=0.999$ and (b) $r_{\rm ini}=1.01$. The broken lines indicate rectilinear filaments for $r_{\rm ini}=1$. These shapes are obtained numerically by solving Eq. (26).

Verification of our theoretical results by experimental and further numerical analyses is an interesting problem and is left for future work.

ACKNOWLEDGMENTS

We would like to thank Osamu Ishihara, Shingo Ishiwata, Hideki Hoshiba, and Katsuhiro Nishinari for providing us many important opinions throughout the course of this work.

[1] J. E. Hackett and P. F. Evans, "Numerical studies of three-dimensional breakdown in trailing vortex wakes," J. Aircr. **14**, 1093 (1977).
[2] C. Y. Soong, C. H. Chyuan, and R. Y. Tzong, "Thermo-flow structure and epitaxial uniformity in large-scale metalorganic chemical vapor deposition reactors with rotating susceptor and inlet flow control," Jpn. J. Appl. Phys., Part 1 **37**, 5823 (1998).
[3] K.-Y. Hsu, L. P. Goss, and W. M. Roquemore, "Characteristics of a trapped vortex combuster," J. Propul. Power **14**, 57 (1998).
[4] G. K. Batchelor, *An Introduction to Fluid Dynamics* (Cambridge University Press, Cambridge, 1967).
[5] R. J. Arms and F. R. Hama, "Localized-induction concept on a curved vortex and motion of an elliptic vortex ring," Phys. Fluids **4**, 28 (1961).
[6] Lord Kelvin, *Mathematical and Physical Papers* (Cambridge University Press, Cambridge, 1880), Vol. 5, p. 152.
[7] H. Hasimoto, "Motion of a vortex filament and its relation to Elastica," J. Phys. Soc. Jpn. **31**, 293 (1971).
[8] H. Hasimoto, "A soliton on a vortex filament," J. Fluid Mech. **51**, 447 (1972).
[9] S. Kida, "A vortex filament without change its form," J. Fluid Mech. **112**, 397 (1981).
[10] S. Fukumoto, "Stationary configurations of a vortex filament in background flows," Proc. R. Soc. London, Ser. A **453**, 1205 (1997).
[11] S. C. Crow, "Stability theory for a pair of trailing vortices," AIAA J. **8**, 2172 (1970).
[12] J. Jimenez, "Stability of a pair of co-rotating vortices," Phys. Fluids **18**, 1580 (1975).
[13] R. Takaki and A. K. M. F. Hussain, "Dynamics of entangled vortex filaments," Phys. Fluids **27**, 761 (1984).
[14] K. Ohtsuka, R. Takaki, and S. Watanabe, "Dynamics of the local entanglement on two vortex filaments described by the Korteweg-de Vries equation," Phys. Fluids **15**, 1065 (2003).
[15] S. Watanabe (unpublished).